Human Molecular Genetics, 2015, Vol. 24, No. 19 5388–5403

doi: 10.1093/hmg/ddv262
Advance Access Publication Date: 9 July 2015
Original Article

ORIGINAL ARTICLE

Phospholipid transfer protein (PLTP) deficiency accelerates memory dysfunction through altering amyloid precursor protein (APP) processing in a mouse model of Alzheimer's disease

Yawei Tong[1], Yang Sun[1], Xiaosheng Tian[1], Ting Zhou[1], Hecheng Wang[1], Tao Zhang[1], Rui Zhan[1], Lei Zhao[1], Bolati Kuerban[1], Zhengqian Li[4], Qiudian Wang[1], Yinglan Jin[1], Dongsheng Fan[3,*], Xiangyang Guo[4], Hongbin Han[5,*], Shucun Qin[2,*] and Dehua Chui[1,3,*]

[1]Neuroscience Research Institute and Department of Neurobiology, Key Laboratory for Neuroscience, Ministry of Education and Ministry of Public Health, Health Science Center, Peking University, Beijing, China, [2]Key Laboratory of Atherosclerosis in Universities of Shandong, Institute of Atherosclerosis, Taishan Medical University, Taian, China, [3]Department of Neurology, [4]Department of Anesthesiology and [5]Department of Radiology, Peking University Third Hospital, Beijing, China

*To whom correspondence should be addressed at: Neuroscience Research Institute, Peking University Health Science Center, 38 Xueyuan Road, Hai Dian District, 100191 Beijing, China. Tel: +86 1082802920; Fax: +86 1082805221; Email: dchui@bjmu.edu.cn (D.C.); dsfan@sina.com (D.F.); hanhongbin@bjmu.edu.cn (H.H.); sucunqin@hotmail.com (S.Q.)

Abstract

Phospholipid transfer protein (PLTP) is a widely expressed lipid transfer protein participating in the transport of cholesterol and other lipids in the plasma and peripheral tissues. Recently, elevated amyloid β (Aβ) in young and aged PLTP-deficient brains had been reported. However, the role of PLTP in amyloid precursor protein (APP) processing and Alzheimer's disease (AD) pathology remains elusive. Here we first found that deficiency of PLTP accelerated memory dysfunction in APP/PS1ΔE9 AD model mice at the age of 3 months. Further characterization showed that PLTP deficiency increased soluble Aβ peptides, and intracellular accumulation of Aβ was illustrated, which might be due to disrupted APP turnover and the enhanced amyloidogenic pathway. Besides, reduced brain-derived neurotrophic factor (BDNF) was found in PLTP-deficient APP/PS1ΔE9 mice, and the BDNF level was negatively correlated with Aβ42 content, instead of Aβ40 content. In addition, autophagic dysfunction was found in the PLTP-deficient APP/PS1ΔE9 mice. Our data presented a novel model to link phospholipid metabolism to APP processing and also suggested that PLTP played an important role in Aβ metabolism and would be useful to further elucidate functions of PLTP in AD susceptibility.

Received: May 1, 2015. **Revised:** June 22, 2015. **Accepted:** July 6, 2015

Introduction

Amyloid β (Aβ) is thought to begin accumulating in the brain many years before the onset of clinical impairment in patients with Alzheimer's disease (AD) (1). The underlying amyloid precursor protein (APP) processing has been strongly implicated in the pathological progress of AD (2). APP undergoes the amyloidogenic pathway by β-secretase BACE1 (β-site APP cleaving enzyme-1) and γ-secretase complex to generate the hydrophobic Aβ peptides, the main constituent of extracellular amyloid plaques in AD (3). This pathway commences intracellularly, as APP is internalized from the cell surface to endosomal compartments where β- and γ-secretases act (4). Besides the Aβ plaque-associated learning deficits, several studies have involved intraneuronal Aβ in the toxic processes in AD (5), and early onset of memory dysfunction may be caused by the accumulation of Aβ within neurons (6).

Phospholipid transfer protein (PLTP), one of the key proteins in lipid and lipoprotein metabolism peripherally, is also widely expressed in the central nervous system (7). PLTP plays a key role in lipid metabolism with its functions of lipid transfer (8) and proteolytic (9) properties extracellularly. Meanwhile, PLTP is present in the nucleus with phospholipid transfer activity (10), indicating its intracellular functions. Nevertheless, reports of PLTP in the central nervous system are limited by now. Patients of AD with no apparent or only mild neuronal loss have significantly higher levels of PLTP in brain tissue, which might reflect a functional response to the metabolic changes occurring in AD pathology (7). Recently, elevated Aβ and reduced synaptic function marker synaptophysin had been found in PLTP-deficient mice (11,12). Phenotype of PLTP-deficient old mice was associated with impaired recognition (11). However, the role of PLTP in APP processing-related learning and memory is poorly understood.

To determine effects of PLTP deficiency on memory function and APP processing *in vivo*, we used APP/PS1ΔE9 mice and crossed them on PLTP knockout background. We first found that deficiency of PLTP in APP/PS1ΔE9 mice accelerated memory deficits at the age of 3 months. Further characterization showed that PLTP deficiency increased intracellular accumulation of Aβ with disrupted APP trafficking and processing. Our results suggested a new insight on APP processing and indicated the important role of PLTP, which was involved in early onset of AD.

Results

PLTP deficiency accelerated memory dysfunction in APP/PS1ΔE9 mice

Previous studies have demonstrated the cognitive impairment of PLTP knockout mice (PLTPko mice) at the approximate age of 12 months compared with wild-type control (11) and 6 months with the APP/PS1ΔE9 AD model mice (APP mice) (13). To determine how deficiency of PLTP contributed to the memory dysfunction observed in AD, we crossed PLTPko mice to APP mice and used Morris water maze (MWM) test to outline the spatial learning and memory retention of PLTP-deficient APP mice (APP&PLTPko mice). Surprisingly, accelerated memory dysfunction was found at the age of 3 months in APP&PLTPko mice, compared with WT, PLTPko and even APP mice (Fig. 1).

During the acquisition phase of MWM test, all mice improved their performance with daily training, exemplified by the escape latency (Fig. 1A) and path length (Fig. 1B). The deletion of PLTP did not affect the cognitive performance in the non-transgenic mice at this age (WT versus PLTPko), which was in accordance with the previous report (12). In contrast, PLTP deficiency significantly worsened the acquisition of spatial memory in the APP transgenic mice [for escape latency, $F_{(1,120)} = 3.959$ and $P = 0.0489$; for path length, $F_{(1,120)} = 3.945$ and $P = 0.0493$]. For each trial day, APP&PLTPko mice learned the task significantly slower than WT animals, specifically on the 3rd to 6th trial day, whereas APP mice performed indistinguishably with WT mice on all days (Fig. 1A and B). Figure 1C showed the performance during the probe trial of MWM test and demonstrated that PLTP deficiency caused significant deficits in memory retention in APP mice. APP&PLTPko mice spent significantly less time and crossed less than WT, PLTPko and APP mice in the quadrant in which the platform was previously located (Fig. 1C), whereas APP, PLTPko and WT mice showed no significant difference between each other, suggesting impaired ability of APP&PLTPko mice to form spatial memory. In general, the results from the MWM test demonstrated that deficiency of mouse PLTP significantly accelerated memory deficits in transgenic mice expressing human APP gene but not in wild-type mice at this young age.

Spatial memory of all mice was also evaluated in a dry condition via the Y maze test. As shown in Figure 1D and E, PLTP deficiency also accelerated memory dysfunction in APP/PS1ΔE9 mice, but did not affect wild-type mice at the age of 3 months (fewer entries into the novel arm), consistent with the results obtained from the MWM test.

PLTP deficiency aggravated the intracellular accumulation of Aβ in APP/PS1ΔE9 mice

Effects of PLTP deficiency on the processing of overexpressed APP in brains of APP mice might be responsible for the observed memory deficits in 3-month-old APP&PLTPko mice. First, we detected the levels of Aβ peptides in the brain, which were thought to be critical for the memory dysfunction in AD (14). Triton X-soluble Aβ peptides were measured by enzyme-linked immunosorbent assay (ELISA) (Fig. 2A), and we found that the levels of Aβ42 in the brains of APP&PLTPko mice were markedly elevated compared with APP mice, respectively (2.04 ± 0.17 versus 1.21 ± 0.12 pmol/mg wet brain, $P = 0.004$). Aβ40 content was also increased in the brain of APP&PLTPko mice, compared with APP mice (2.03 ± 0.14 versus 1.43 ± 0.12 pmol/mg wet brain, $P = 0.011$). The levels of Aβ peptides were also increased in PLTPko mice, compared with WT mice (Fig. 2A). Furthermore, there was a negative correlation between the level of Aβ peptides in the brain and probe trial performance of mice in all groups, suggesting a causative relation between the two (Fig. 2B). Additionally, both Aβ42 and Aβ40 contents were negatively correlated with the probe trial performance of APP and APP&PLTPko mice (Fig. 2C). These results indicated that the elevation of Aβ peptides might be the primary cause of cognitive impairment in PLTP-deficient APP mice.

In order to determine the extent or pattern of the amyloid accumulation in the brains of mice, brain sections of four groups were subjected to immunocytochemical analysis and confocal microscopy. It has been previously demonstrated that the amyloid plaque deposits first started to appear at the age of 6 months in this AD model (15,16), and there is neither diffuse nor fibrillar plaque deposition in the brains at 3 months of age (17). Expectedly, no typical senile plaques were observed in the cerebral cortex and hippocampus of all 3-month-old mice. At this age, APP mice showed intracellular Aβ pathology in the hippocampus and cortex, and APP&PLTPko mice performed strikingly worse (Fig. 2D). With the confocal microscopy, Aβ accumulation was visualized

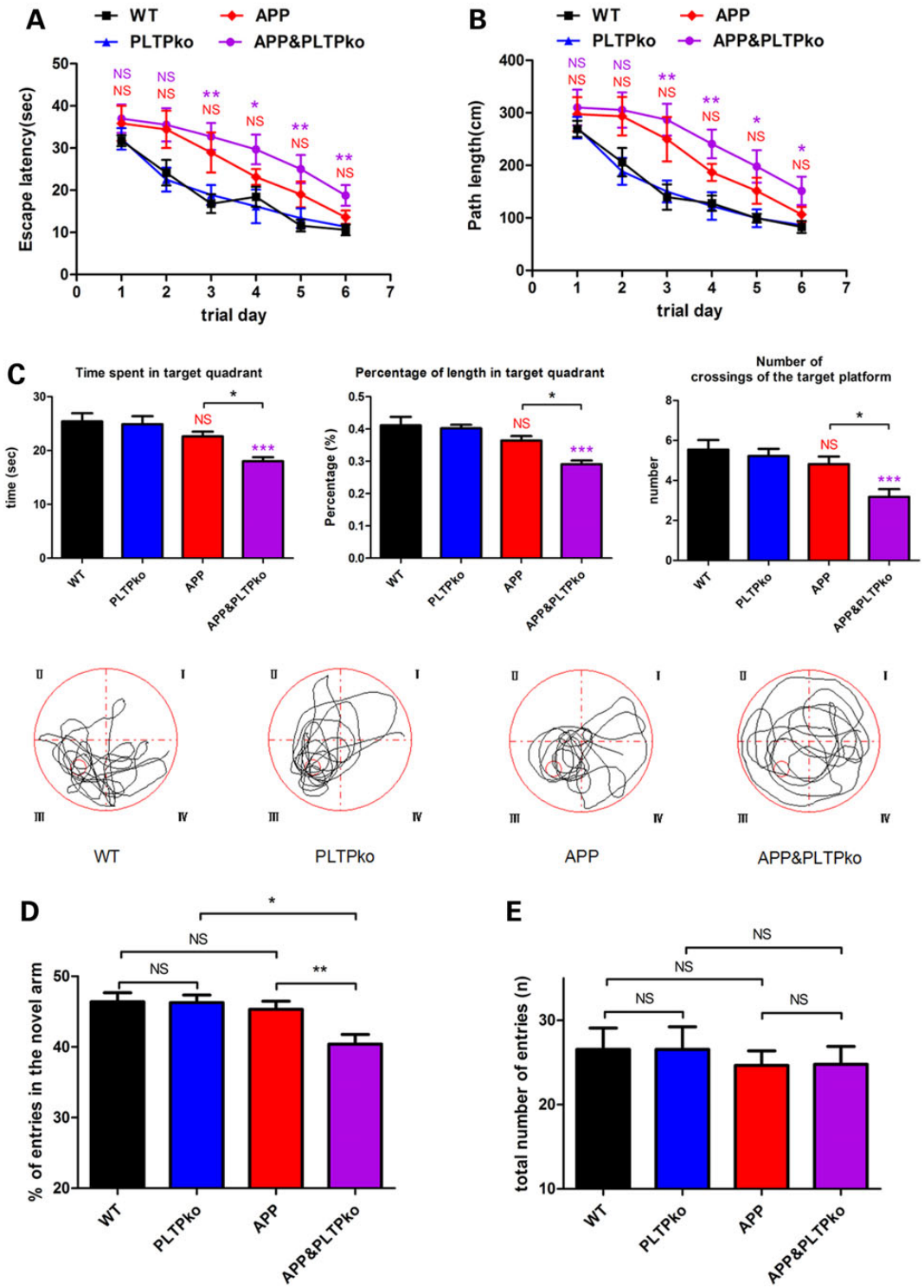

Figure 1. PLTP deficiency accelerated memory dysfunction in APP/PS1ΔE9 mice but did not affect wild-type mice at the age of 3 months. (**A**) Escape latency scores of the MWM test represented the average acquisition time to find the platform per trial day. For each trial day, APP mice performed indistinguishably with WT mice on all days, whereas APP&PLTPko mice performed significantly worse than WT animals on the 3rd to 6th trial days (two-way ANOVA with a Tukey's *post hoc* test). There was a significant group effect on escape latency between the APP&PLTPko mice and APP mice [$F_{(1,120)} = 3.959$, $P = 0.0489$]. (**B**) Path length scores of the MWM test represented the average distance swum to find the platform per trial day. APP&PLTPko mice performed significantly worse than WT animals on the 3rd to 6th trial days (one-way ANOVA with a Tukey's *post hoc* test). There was also a significant group effect on path length between the APP&PLTPko and APP mice [$F_{(1,120)} = 3.945$, $P = 0.0493$]. (**C**) During the probe trial of the MWM test, time spent in the target quadrant, percentage of length in the target quadrant and number of crossings of the target platform were calculated, and representative swim paths were shown. APP&PLTPko mice spent less time, swam less length in the target quadrant and crossed less in the target platform than WT mice ($P < 0.001$) and APP mice ($P < 0.05$). APP mice, PLTPko mice and WT mice showed no difference between each other. (**D**) Percentage of entries in the novel arm and (**E**) the total number of entries (respectively) during the test sessions of Y-maze test were shown. Analysis was performed by one-way ANOVA followed by Tukey's *post hoc* test. Bars represent means ± SEM; $n = 12$ WT mice, $n = 9$ PLTPko mice, $n = 11$ APP mice and $n = 11$ APP&PLTPko mice. NS, no significance; $^{*}P < 0.05$; $^{**}P < 0.01$ and $^{***}P < 0.001$ (red: APP mice versus WT mice and purple: APP&PLTPko mice versus WT mice).

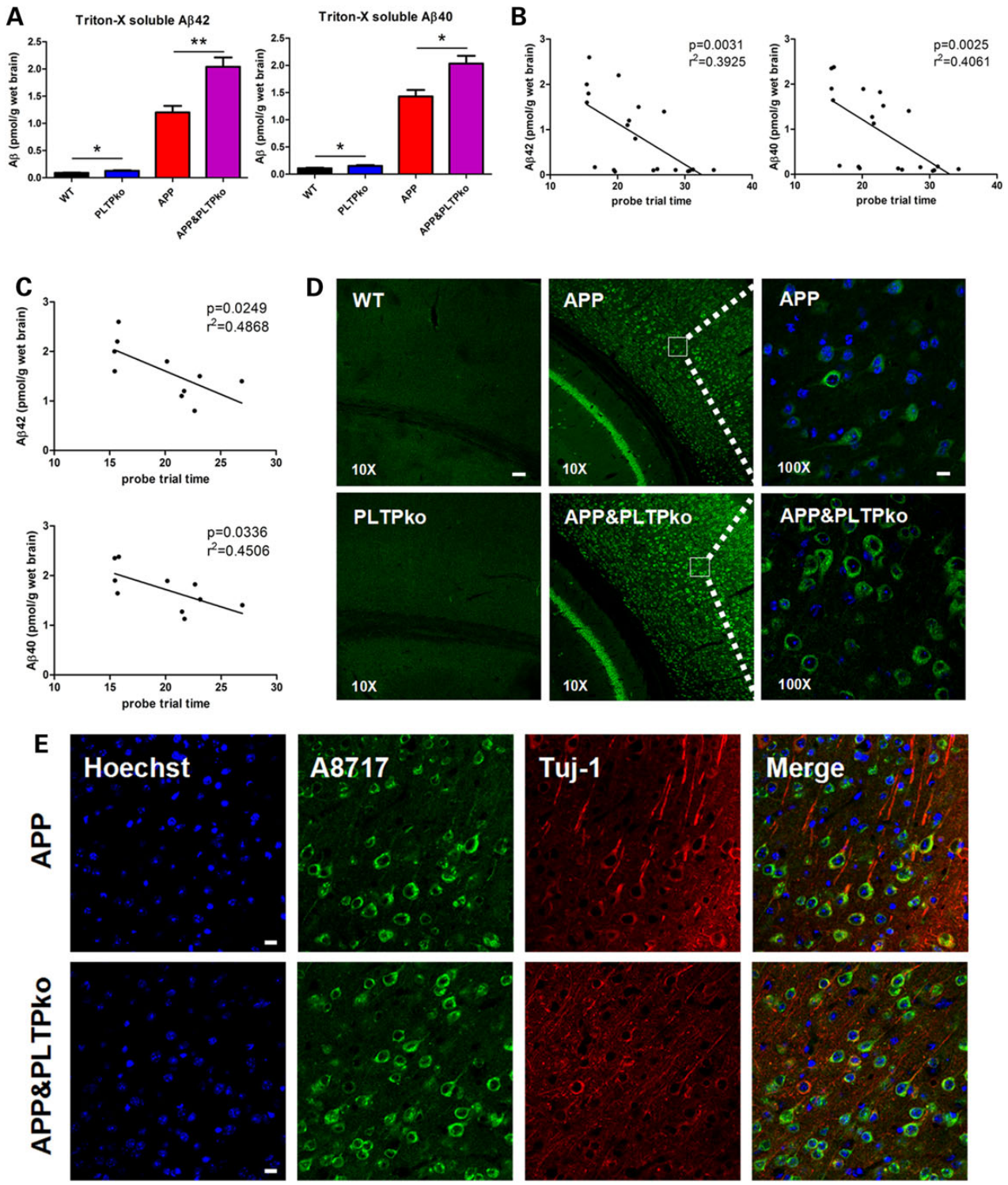

Figure 2. Effects of PLTP deficiency on Aβ pathology in 3-month-old mice. (**A**) Quantification of brain Aβ42 and Aβ40 concentrations in WT, PLTPko, APP and APP&PLTPko mice. Triton X-soluble Aβ peptides were measured by ELISA. Data are expressed as mean ± SEM (error bars) ($n = 5$ for each group). Statistical significance values were calculated with the unpaired Student's *t*-test. *$P < 0.05$ and **$P < 0.01$. (**B**) Graphical representation of partial regression for Aβ42 and Aβ40 with the corresponding probe trial time of four group mice ($n = 20$) (correlation analysis). (**C**) Graphical representation of partial regression for Aβ42 and Aβ40 with the corresponding probe trial time of APP and APP&PLTPko mice ($n = 10$) (correlation analysis). (**D**) Confocal microscopic analysis of Aβ pathology in WT, PLTPko, APP and APP&PLTPko mice. Aβ was hardly detected in WT and PLTPko mice. APP and APP&PLTPko mice displayed intracellular Aβ pathology in the cortex and hippocampus but no extracellular Aβ deposition. APP&PLTPko mice showed elevated Aβ immunoreactivity than APP mice. Green, 6E10 staining; blue, nuclear Hoechst staining. Magnification: 10×, scale bar 100 μm and 100×, scale bar 10 μm. (**E**) Confocal microscopic analysis of APP and its derivatives with the A8717 antibody (green) in APP and APP&PLTPko mice. The antibody for neuronal class III β-tubulin (Tuj-1, red) was co-stained. No distinguishable changes in immunoreactivities for A8717 could be seen between the two groups. Scale bar 10 μm.

diffusely throughout the neuronal cytoplasm in the hippocampus and cortex of APP&PLTPko mice. The A8717 antibody was also used (Fig. 2E), which could detect APP and its derivatives but not Aβ. There were no distinguishable changes in immunoreactivities for A8717 between the APP mice and APP&PLTPko mice (Fig. 2E). The data confirmed that the elevated Aβ peptides in PLTP-deficient APP mice were predominantly present intracellularly, which might lead to neuronal dysfunction and induce memory deficits.

Additionally, we evaluated effects of PLTP deficiency on senile plaques at later ages in the APP transgenic mice (Supplementary Material, Fig. S1). APP mice began to exhibit amyloid plaques at the age of 6 months, and PLTP-deficient APP mice exhibited sharper plaques. Up to 12 months, PLTP deficiency aggravated the amyloid plaques more prominently and diffusely in the mouse brain. These data further stressed the importance of PLTP in AD progression.

We also investigated the effect of PLTP deficiency on other APP metabolite levels in APP mice. As shown in Figure 3A, increased CTFβ, the β-secretase-cleaved C-terminal fragment of APP, was found in APP&PLTPko mice, whereas full-length APP (flAPP) and CTFα had no change, compared with APP mice. In addition, we

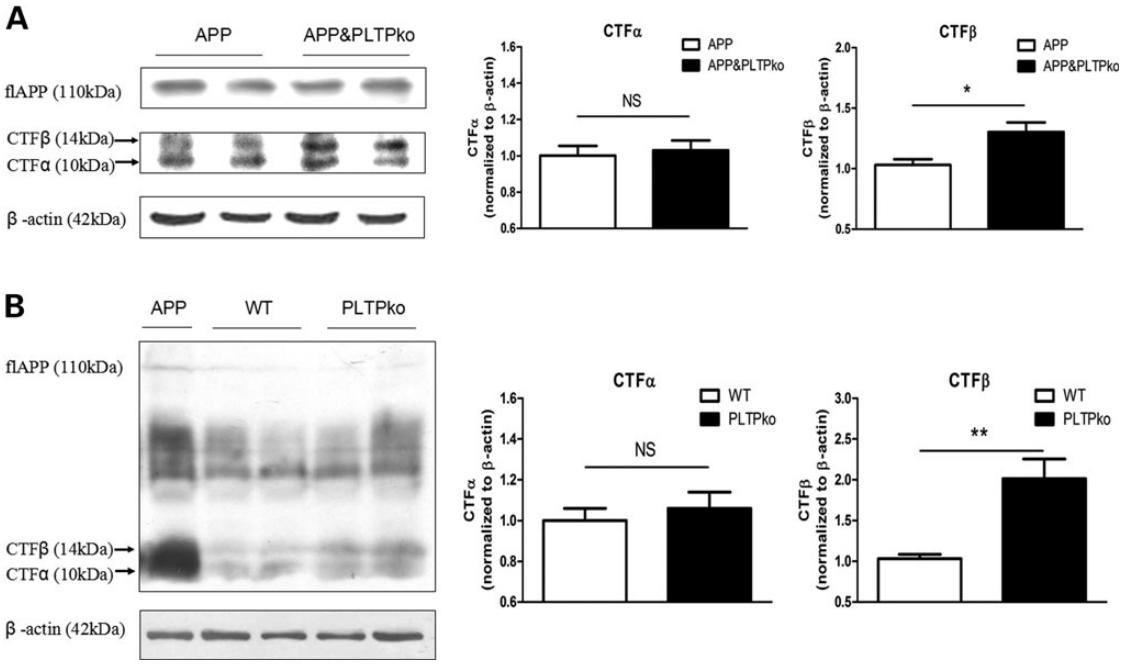

Figure 3. Effects of PLTP deficiency on cleaved products of APP in 3-month-old mice. (**A**) Representative western blots and quantitative analysis of flAPP and CTFα/β for APP processing and β-actin in brains of APP and APP&PLTPko mice. (**B**) With the protein from APP mice as a positive control, representative western blots and quantitative analysis of flAPP and CTFα/β for APP processing, and β-actin in brains of WT and PLTPko mice were shown. Data are mean ± SEM (error bars) ($n = 5$ for each group). Statistical significance values were calculated with the unpaired Student's *t*-test. NS, no significance; $^{*}P < 0.05$ and $^{**}P < 0.01$. CTFβ, the β-secretase-cleaved C-terminal fragment of APP; CTFα, the α-secretase-cleaved C-terminal fragment of APP.

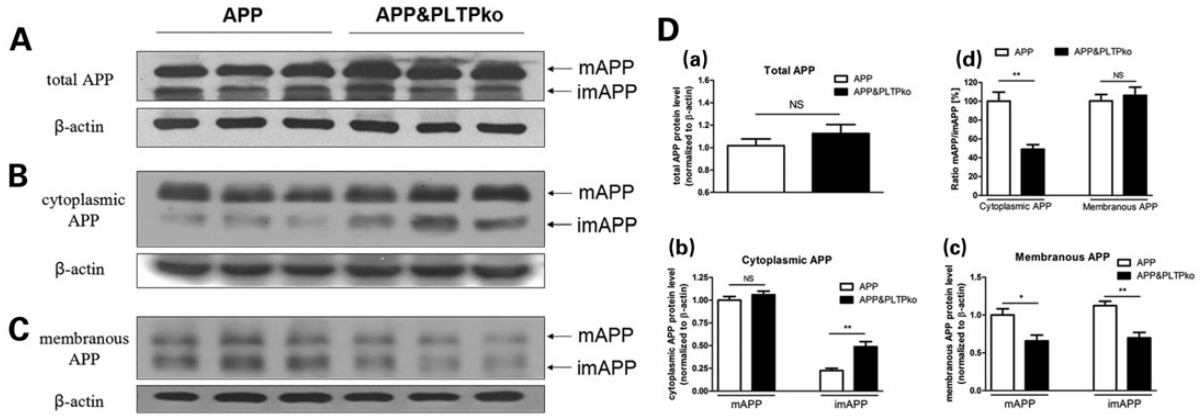

Figure 4. Effects of PLTP deficiency on APP turnover in APP/PS1ΔE9 mice. (**A**) Total protein was collected from homogenated brain and was analyzed for total mature and immature APP with the WO2 antibody and β-actin as a loading control in APP and APP&PLTPko mice. (**B**) In the cytoplasmic extracts and (**C**) in the membranous extracts, mature and immature APP were also detected with the WO2 antibody. The arrows indicate bands corresponding to mature APP (mAPP) and immature APP (imAPP). β-actin was used as a loading control in each extract. (**D**) Quantitative analysis for total APP (a), cytoplasmic (b) and membranous (c) mAPP and imAPP, and the ratio of the mature to immature APP levels (d). Data are mean ± SEM (error bars) ($n = 6$ for each group). Statistical significance values were calculated with the unpaired Student's *t*-test. NS, no significance; $^{*}P < 0.05$ and $^{**}P < 0.01$.

also tried to detect the CTFα/β in wild-type mice, although there were much fewer CTFs under the non-transgenic background. With the protein from APP mice as a positive control, after longer exposure in western blot analysis, the CTFs were measured (Fig. 3B). Similar to the results in APP mice, PLTP deficiency did not change the level of CTFα, but increased the level of CTFβ in WT mice significantly. These data indicated that PLTP deficiency did not affect the non-amyloidogenic pathway, but enhanced the amyloidogenic pathway of APP.

PLTP deficiency disrupted APP turnover in APP/PS1ΔE9 mice

As APP processing depends on its exposure to the different secretases present on the cell surface or in the cytoplasm, we tested whether PLTP regulated APP processing via affecting its distribution. It has been demonstrated that the non-amyloidogenic processing occurs mainly at the cell surface, where α-secretases are present (18), and β- and γ-secretases predominantly localize intracellularly (19). We examined the expression of APP protein from cell surface to cytoplasm by western blot, which reflected the capacity of amyloidogenic cleavage. Total protein and proteins from membranous and cytoplasmic extracts were prepared from the brains of mice. Though increased in APP&PLTPko mice, total APP (including mature and immature forms) in total protein was indistinguishable between the APP and APP&PLTPko mice (Fig. 4A and Da). In addition, the mRNA level of mutated human APP was not changed between the two groups (data not shown). Further in the cytoplasmic extracts, it was surprising to find that the immature form of APP was significantly elevated, but the mature form of APP had no change (Fig. 4B and Db), and the ratio of mature APP to immature APP (m/imAPP) was significantly decreased (Fig. 4Dd) in APP&PLTPko mice, compared with APP mice. In the meanwhile, both mature APP and immature APP were reduced in the membranous extracts of APP&PLTPko mice (Fig. 4C and Dc), but the m/imAPP ratio was not changed (Fig. 4Dd). These data suggested that PLTP deficiency could disrupt the maturation and/or distribution of APP, which accounted for the processing of APP.

PLTP deficiency enhanced the endocytic pathway for APP processing in APP/PS1ΔE9 mice

Intracellular APP underwent the endocytic pathway with β- and γ-cleavage, mainly in endosomes, and then generated Aβ peptides (20). Impairment of APP trafficking and the retention of APP may elicit the induction of the endocytic pathway, by which excess APP can be metabolized and Aβ peptides are generated. In support of this speculation, we found that both early (Fig. 5A) and late endosomes (Fig. 5B) were much more strongly

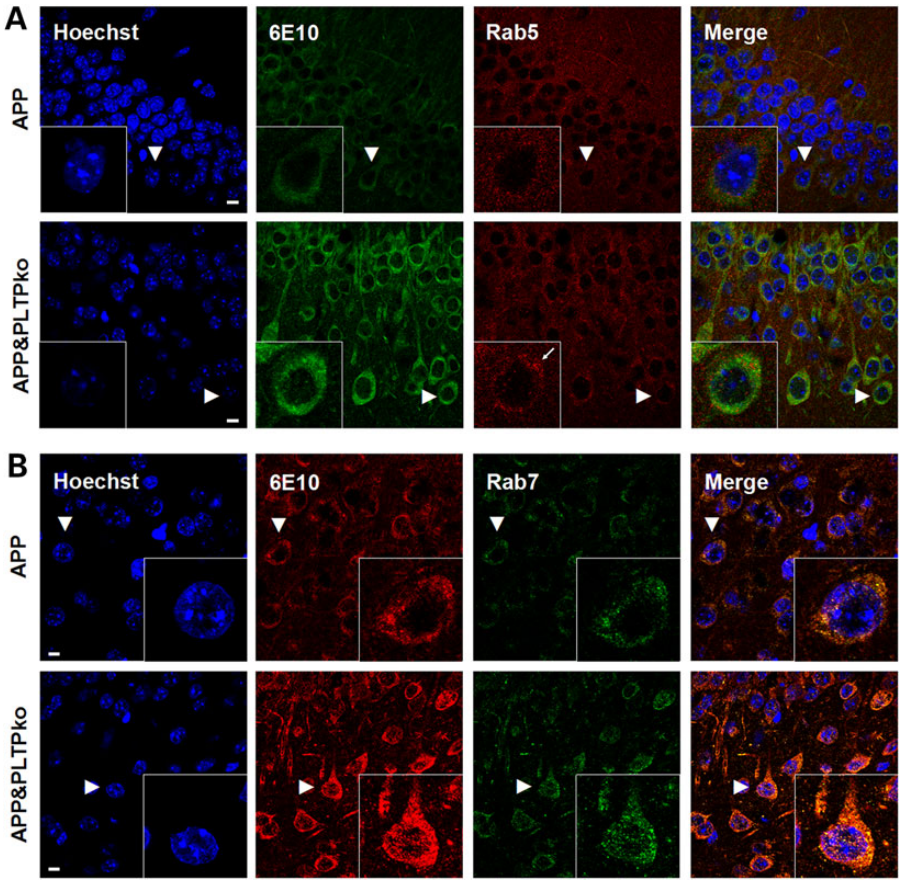

Figure 5. Effects of PLTP deficiency on the endocytic pathway with the intracellular accumulation of Aβ. Brain sections from APP and APP&PLTPko mice were permeabilized, blocked and co-stained with the indicated antibodies. (**A**) Representative immunofluorescent microphotographs of brain sections co-stained with Aβ (6E10, green) and an anti-Rab5 antibody for early endosomes (red). (**B**) Representative immunofluorescent microphotographs of brain sections stained with Aβ (6E10, red) and an anti-Rab7 antibody for late endosomes (green). Remarkable enrichment of immunoreactivities for Rab5 and Rab7 was visualized in APP&PLTPko mice. Blue, nuclear Hoechst staining. Scale bar 10 μm.

induced in the brains of APP&PLTPko mice, compared with APP mice. Aβ accumulation was more prominent in late endosomes in both mice (Fig. 5B). Thus, the enhanced endocytic pathway could be responsible for the excessive production of Aβ.

PLTP deficiency up-regulated enzymes in the amyloidogenic pathway of APP

Our data mentioned earlier showed that deficiency of PLTP accelerated Aβ generation. To identify the underlying mechanism, we investigated the effects of PLTP knockout on the levels of three key enzymes in APP processing, namely, α-secretase ADAM10 (a disintegrin and metalloprotease 10), beta-site amyloid precursor protein cleaving enzyme 1 (BACE1) and presenilin1 (PS1) in APP mice and APP&PLTPko mice, and we found that total ADAM10 had no change between the two groups, whereas a highly significant increase by 116% of BACE1 and a slight but significant increase by 36% of PS1 were detected in APP&PLTPko mice (Fig. 6A and B). Gene expression analyzed by mRNA showed corresponding results (Fig. 6C), which suggested a novel role of PLTP involved in regulating transcription of several proteins. We also subjected the supernatant of brain tissues to β-secretase activity assay, and elevated β-secretase activity was found in APP&PLTPko mice, compared with APP mice (Fig. 6D). With PLTP RNAi in N2a neuroblastoma cells expressing Swedish mutant APP (N2a-APPsw), we treated the cultured cells with beta-secretase inhibitor GRL-8234 (Supplementary Material, Fig. S2) and found that the administration of beta-secretase inhibitor could reduce the elevated Aβ levels in PLTP RNAi cells. Combined with increased CTFβ and Aβ peptides, it could be concluded that PLTP deficiency would induce the amyloidogenic pathway of APP and increase the neurotoxic Aβ product.

PLTP deficiency down-regulated brain-derived neurotrophic factor

A large number of reports have indicated that expressions of the brain-derived neurotrophic factor (BDNF) are decreased in patients with AD (21–23), and Aβ peptides, especially the Aβ42, may account for the decreased BDNF (24,25). To examine whether deficiency of PLTP and/or intracellular accumulation of Aβ peptides alters BDNF expression, we performed immunoblotting tests for protein levels of BDNF in the mouse brains. Indeed, the BNDF level was significantly reduced by 44% in APP&PLTPko mice, compared with APP mice (Fig. 7A, $P = 0.0025$). Non-parametric correlation analysis demonstrated a positive correlation between BDNF in brain and the time spent in the target quadrant during the probe trial (Fig. 7B, $P = 0.0298$, $r^2 = 0.4652$). Further, the correlation between BDNF and the corresponding Aβ peptides was determined. Interestingly, BDNF was significantly negatively correlated with the Aβ42 level (Fig. 7C, $P = 0.0096$, $r^2 = 0.5890$), but had no correlation with the Aβ40 level (Fig. 7D, $P = 0.2697$, $r^2 = 0.1495$). These data suggested that the elevated Aβ42 level by PLTP deficiency might be involved in the regulation of BNDF protein level.

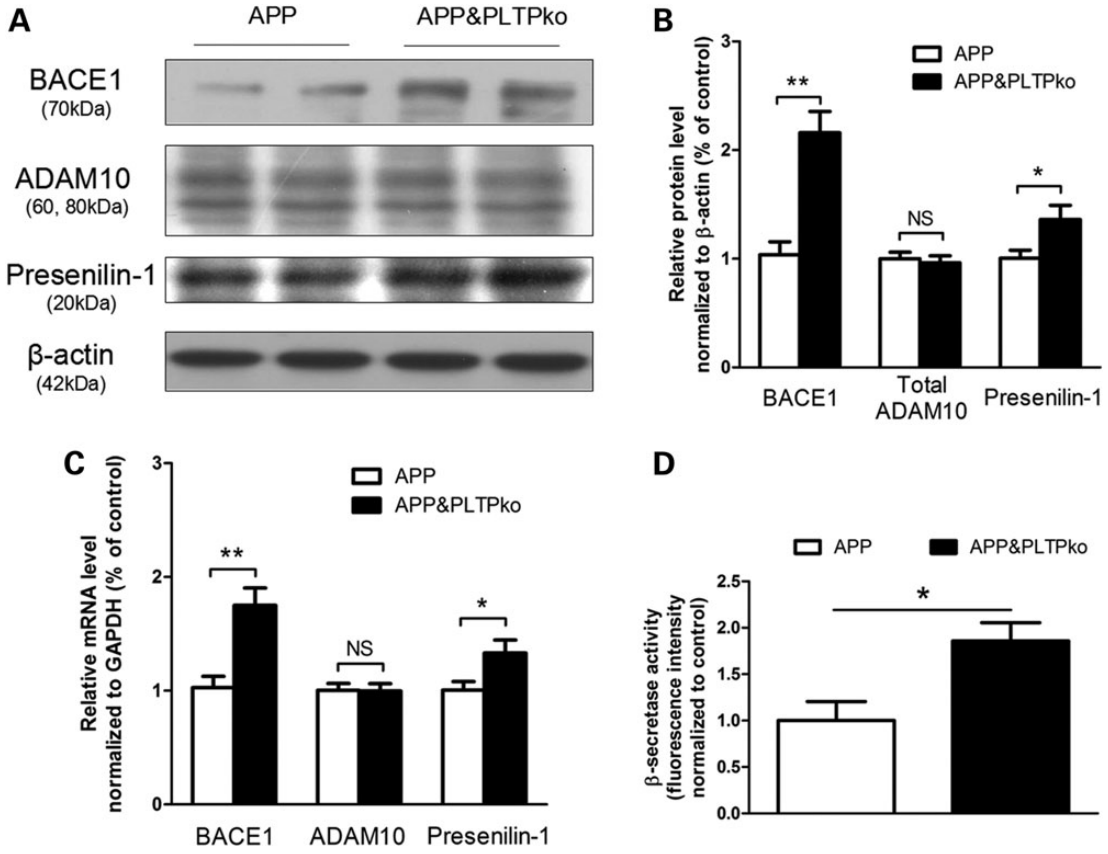

Figure 6. Effects of PLTP deficiency on key enzymes for APP processing. Representative western blots (**A**) and quantitative analysis (**B**) of BACE1, ADAM10, presenilin-1 and β-actin in brains of APP and APP&PLTPko mice were shown. (**C**) mRNA levels of BACE1, ADAM10 and presenilin-1 were quantitated by RT–PCR and normalized to GAPDH controls and expressed as ratios of control levels. Data are mean ± SEM (error bars) ($n = 5$ for each group). (**D**) BACE1 activity in brain extracts was assayed, following the manufacturer's instructions. Data are mean ± SEM (error bars) ($n = 5$ for each group). Statistical significance values were calculated with the unpaired Student's *t*-test. $^*P < 0.05$ and $^{**}P < 0.01$.

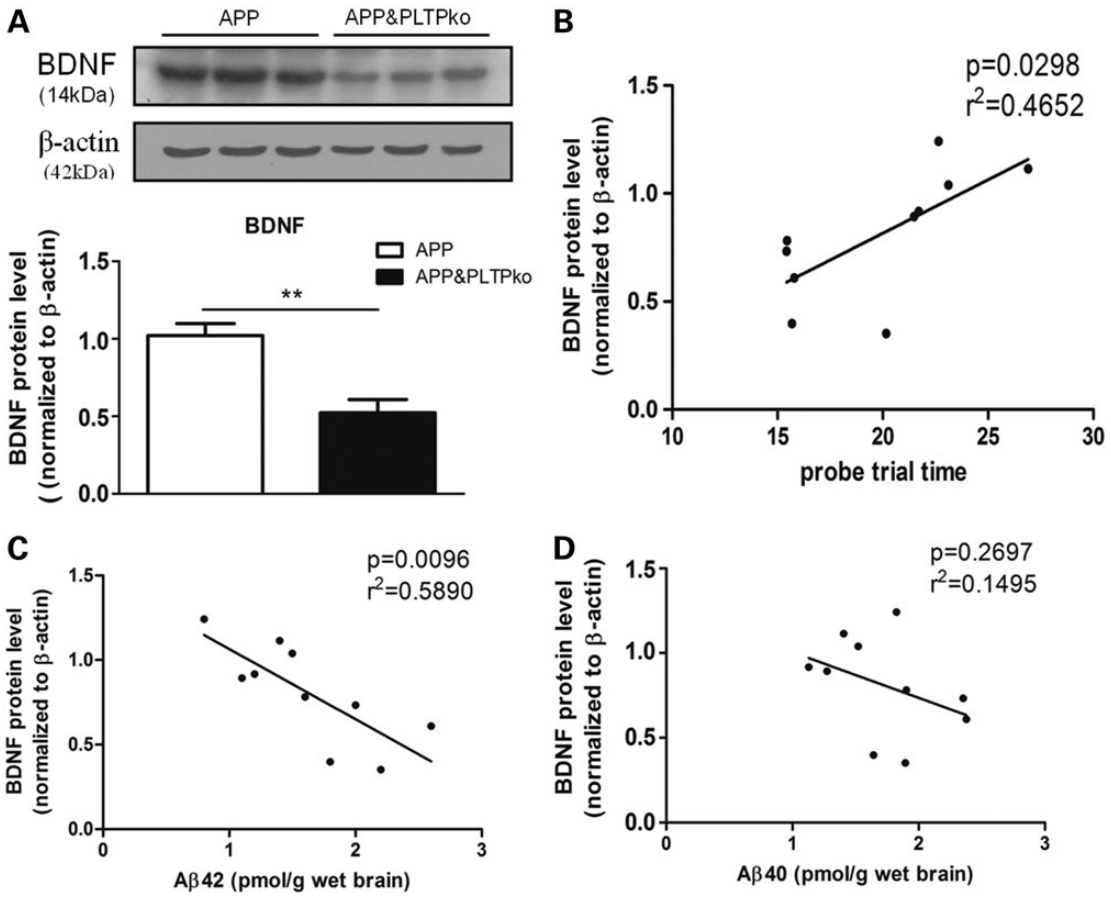

Figure 7. Effects of PLTP deficiency on BDNF levels. (**A**) Representative western blots and quantitative analysis of BNDF and β-actin in brains of APP and APP&PLTPko mice were shown. BNDF protein level was significantly reduced by 44% in APP&PLTPko mice compared with APP mice ($P = 0.0025$ with the unpaired Student's *t*-test). Data are expressed as mean ± SEM (error bars) ($n = 5$ for each group). (**B**) Graphical representation of partial regression for BNDF with the corresponding probe trial time of APP and APP&PLTPko mice ($n = 10$) (correlation analysis). BDNF was positively correlated with the time spent in the target quadrant during the probe trial ($P = 0.0298$ and $r^2 = 0.4652$). (**C** and **D**) Graphical representation of partial regression for BNDF with the corresponding Aβ42 and Aβ40 levels of APP and APP&PLTPko mice ($n = 10$) (correlation analysis). BDNF was negatively correlated with the Aβ42 level ($P = 0.0096$ and $r^2 = 0.5890$), but had no correlation with the Aβ40 level ($P = 0.2697$ and $r^2 = 0.1495$).

Interaction between PLTP and APP

In order to elucidate the probable mechanism of abnormal APP turnover by PLTP deficiency, we sought to examine the potential of PLTP and APP to interact. It was surprising that APP co-immunoprecipitated with PLTP from mouse brain extracts in APP mice (Fig. 8A). APP was also observed to co-immunoprecipitate with PLTP in these mice (Fig. 8B). In addition, immunofluorescence microscopy showed that PLTP was predominantly co-localized with APP in the brain of APP mice (Fig. 8C). In order to get better visualization, cultured mouse N2a neuroblastoma cells expressing Swedish mutant APP were subjected to confocal microscopy analysis for PLTP and APP. Although APP and PLTP did have distinct staining patterns, significant co-localization of PLTP with APP could be evidenced from the merged image (Fig. 8D). Additionally, compared with PLTP RNAi-transfected N2a-APPsw cells, we treated N2a-APPsw cells with the PLTP activity inhibitor cpd A (Supplementary Material, Fig. S2) and found that the levels of total intracellular Aβ were sharply increased by PLTP RNAi, but the PLTP inhibitor had no significant effect, which suggested that the PLTP protein itself should be more critical for its role in Aβ metabolism. These data indicated a probable role of PLTP in regulating the bioavailability of APP, such as affecting its distribution via the cross-linked interaction.

PLTP deficiency impaired autophagic function in APP/PS1ΔE9 mice

Neuronal macroautophagy has been found early in AD patients and before Aβ deposits extracellularly in the AD mouse model (26), which accounts for the degradation of intracellular Aβ (27). In order to unfold whether the ability for the clearance of Aβ was changed via PLTP deficiency, we examined the protein levels of p62 and LC3B for the general autophagic function. Interestingly, there was a significant increase in p62 protein levels in APP&PLTPko mice, compared with APP mice (Fig. 9A). The accumulation of p62 inclusion was further visualized by p62 immunofluorescence in the PLTP-deficient APP mice (Fig. 9B). The ratio of LC3II to LC3I serves as an indicator of autophagic activity, and we found a significant decrease in the ratio of LC3II to LC3I in APP&PLTPko mice, compared with APP mice (Fig. 9A). Immunofluorescence microscopy with co-staining showed that intracellular Aβ was mainly co-localized with LC3, but immunoreactivities for LC3 did not differ significantly between APP and APP&PLTPko mice (Fig. 9C). Additionally, with PLTP RNAi in N2a-APPsw cells, we treated the cultured cells with autophagy inductor rapamycin (Supplementary Material, Fig. S2) and found that the administration of autophagy inductor could reduce the elevated Aβ levels in PLTP RNAi cells. In general, PLTP deficiency

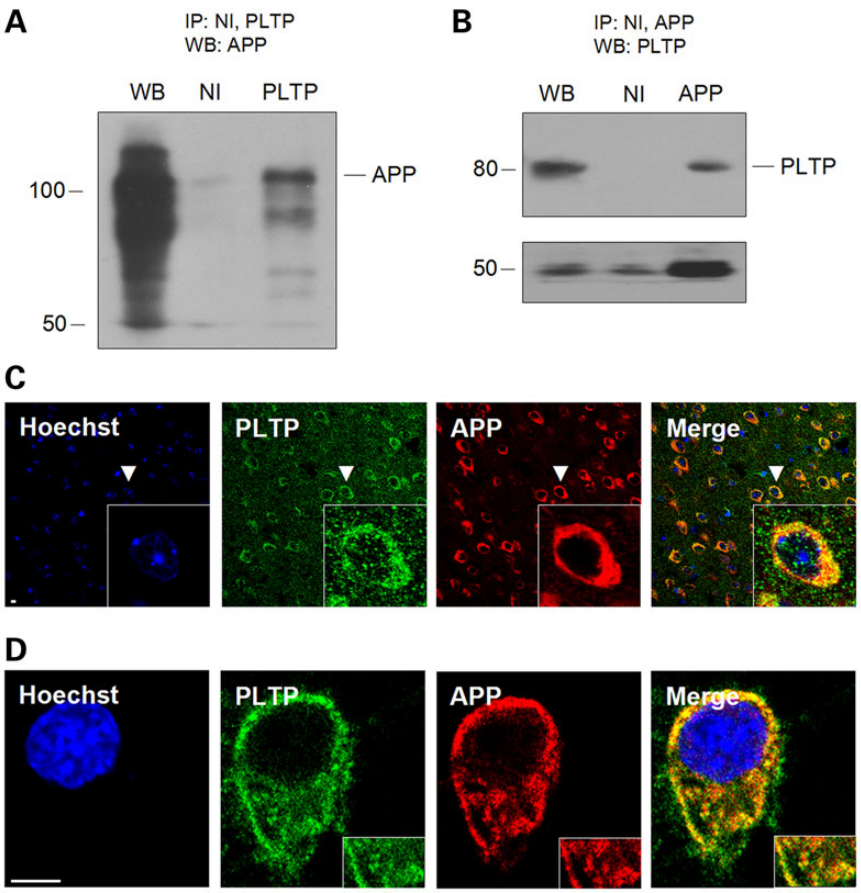

Figure 8. Interaction and co-localization between PLTP and APP. (**A** and **B**) Mouse brain extracts from APP mice were subjected to immunoprecipitation using non-immune IgG (NI) (lane 2), anti-APP 6E10 IgG (APP) or anti-PLTP IgG (PLTP) (lane 3). The immunoprecipitates were analyzed for APP using 6E10 antibody (A) or for PLTP using PLTP antibody (B). Lane 1 represents an immunoblot of brain extract with 6E10 IgG or PLTP IgG, respectively. (**C**) Confocal microscopy analysis for immunoreactivities of PLTP (green) and APP (red) in APP mice. (**D**) Confocal microscopy analysis for immunoreactivities of PLTP (green) and APP (red) in mouse N2a neuroblastoma cells expressing Swedish mutant APP. Insets show enlarged image of the indicated regions. Blue, nuclear Hoechst staining. Scale bar 10 μm.

might impair autophagic function, which could cause disrupted clearance of Aβ.

Impact of PLTP deficiency on brain lipid homeostasis in APP/PS1ΔE9 mice

In order to identify the role of PLTP in modulating brain lipid homeostasis, shotgun lipidomics (28) was used to analyze the main molecular species of lipids from brain extracts of the APP and APP&PLTPko mice. We found that both phosphatidyl ethanolamine and phosphatidylserine were sharply decreased in the APP&PLTPko mice, compared with APP mice at the age of 3 months (Table 1). There was also a slight but significant decrease of phosphatidylinositol (PI) in PLTP-deficient APP mice, whereas most lipid classes had no significant changes (Table 1). These data indicated that PLTP was important for brain lipid homeostasis.

Discussion

PLTP deficiency accelerated memory dysfunction in APP/PS1ΔE9 mice at the non-demented age

As one key protein in lipid metabolism, PLTP has been found to play several roles in the brain with the PLTP knockout mouse model (11,12,29,30). Notably, increased amyloid-β peptides were found in PLTP-deficient mice at both young and old ages (11,12), which raised our interest on the role of PLTP in AD and the specific Aβ-related mechanism. Here with an AD model mice, at the non-demented age of 3 months (17,31), we first found that PLTP deficiency accelerated its memory dysfunction with the behavior tests, suggesting that PLTP was critically involved in learning and memory.

As the 6-month-old APP/PS1ΔE9 mice showed significant AD pathology such as cognitive impairment and Aβ plaque deposition (16), the 3-month-old APP/PS1ΔE9 mice provided an animal model for the early stages of cognitive decline in AD, and deficiency of PLTP might increase its susceptibility to AD. At the early stages of AD, such as mild cognitive impairment (MCI) or earlier, intraneuronal Aβ peptides have been implicated in the toxic processes in AD (32,33), rather than the extracellular Aβ burden (34–36). Several mechanisms underlie the neurotoxicity of intracellular accumulation of Aβ such as endoplasmic reticulum (ER) stress (37,38), disruption of fast axonal transport (39) and synaptic pathology (40). In our study, we found elevated Aβ peptides in brains of PLTP-deficient AD mice, and there was a negative correlation between the level of soluble Aβ peptides in the brain and the probe trial performance of all groups, suggesting a causative role of Aβ in the memory dysfunction. Surprisingly, confocal microscopic analysis showed that PLTP deficiency

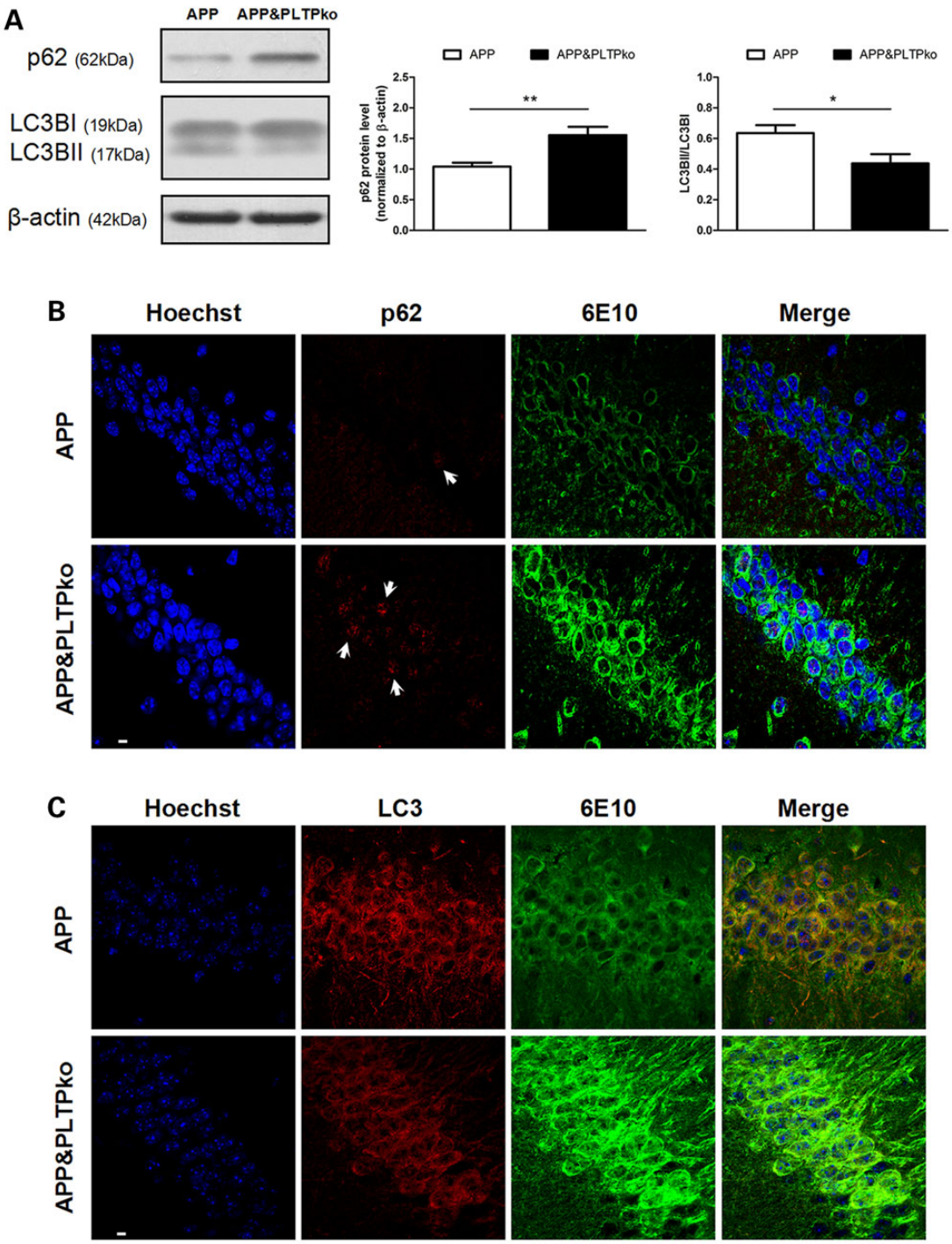

Figure 9. Effects of PLTP deficiency on the autophagy markers. (**A**) Representative western blots and quantitative analysis of p62, LC3B and β-actin in brains of APP and APP&PLTPko mice were shown. The P62 protein level was significantly elevated by 52% in APP&PLTPko mice compared with APP mice ($P = 0.0091$ with the unpaired Student's *t*-test). The ratio of LC3II to LC3I was significantly reduced by 34% in APP&PLTPko mice ($P = 0.0382$ with the unpaired Student's *t*-test). Data are mean ± SEM (error bars) ($n = 5$ for each group). Brain sections from APP mice and APP&PLTPko mice were permeabilized, blocked and co-stained with the indicated antibodies. (**B**) Representative immunofluorescent microphotographs of brain sections stained with Aβ (6E10, green) and an anti-p62 antibody (red). (**C**) Representative immunofluorescent microphotographs of brain sections stained with Aβ (6E10, green) and an anti-LC3 antibody (red). The accumulation of p62 inclusion was visualized in APP&PLTPko mice. Blue, nuclear Hoechst staining. Scale bar 10 μm.

increased intracellular Aβ immunoreactivity in the brain of APP mice, but did not exhibit any extracellular Aβ deposits at the age of 3 months in all mice, which suggested the possible role of PLTP deficiency in intracellular Aβ elevation and the related APP processing.

PLTP deficiency altered APP processing via disrupted APP turnover

The efficiency of APP processing to generate Aβ is greatly affected by its subcellular localization (41), and therefore, it is of central

Table 1. Summary of lipidomics in the brains of APP and APP&PLTPko mice at the age of 3 months

Lipid class	APP mice	APP&PLTPko mice
Triacylglycerol	61.84 ± 4.14	58.84 ± 5.75
Phosphatidylcholine	245.25 ± 13.82	256.74 ± 14.88
Phosphatidyl ethanolamine	266.45 ± 40.42	142.43 ± 23.01***
Phosphatidylserine	193.47 ± 30.16	100.40 ± 22.46***
Phosphatidylinositol	85.75 ± 13.66	67.76 ± 9.70*
Phosphatidylglycerol	22.66 ± 5.85	21.20 ± 5.18
Sphingomyelin	52.40 ± 10.88	42.82 ± 8.89
Free cholesterol	477.65 ± 72.46	435.38 ± 51.64

The data are expressed in nmol/mg of protein and represent mean ± SD of five different mice.
*$P < 0.05$ and ***$P < 0.001$ with the unpaired Student's *t*-test ($n = 5$).

importance to investigate the regulators of trafficking and distribution of APP. APP is synthesized in the ER and modified by the trans-Golgi network during the transit in the secretory pathway en route to the cell surface (42). APP has a relatively short residence time at the cell surface as it either undergoes α-secretase cleavage or becomes internalized into endosomes where β- and γ-secretases cleave. Besides, part of the synthesized APP in the trans-Golgi network would be directly transferred into endosomes for β- and γ-cleavage (20). In our study, it was surprising to found that the immature form of APP was significantly elevated but the mature form of APP had no change in the brain cytoplasmic extracts of PLTP-deficient APP mice, which suggested that imAPP was retained intracellularly via disrupted APP maturation or transport by PLTP deficiency. Combined with decreased mAPP and imAPP in the membranous extracts, mAPP might also be retained in the cytoplasm. One possible explanation for the unchanged cytoplasmic mAPP might be the short half-life of cellular flAPP (43). Excess intracellular APP underwent the amyloidogenic pathway by β-secretase and γ-secretase rapidly and then generated excess CTFβ and Aβ peptides in the neuron. The enhanced endocytic pathway, especially in early and late endosomes, could be a functional response to the excess intracellular APP. In general, the novel turnover of APP caused by PLTP deficiency offered a new insight on APP processing.

Further, co-immunoprecipitation and co-staining experiments revealed that APP was capable of interacting with PLTP. Combined with the data that PLTP deficiency alerted APP turnover, PLTP might be responsible for the trafficking of APP directly, especially its transportation to the cell surface. The mechanism by which PLTP deficiency affected the trafficking and/or processing of APP was not known, but could result from a lack of interaction with APP, which might alter its cellular trafficking, such as enhancing its recycling to endosomal compartments. Indeed, there remain needs for deeper and more comprehensive researches on the role of PLTP in APP processing.

PLTP deficiency enhanced the amyloidogenic pathway for APP processing

After investigating the protein and mRNA levels of three key enzymes in APP processing, we found that ADAM10 was not changed by PLTP deficiency, whereas BACE1 and PS1 were increased in APP&PLTPko mice. The elevated proteins in the amyloidogenic pathway of APP might be a functional response to the excess intracellular APP or be caused by abnormal transcription via PLTP deficiency. PLTP has been demonstrated to be present in the nucleus of several cells and active in lipid transport (10), indicating the probable role of PLTP in the regulation of endonuclear lipids, which can affect cell processes via the endonuclear lipid second messenger signaling (44,45). PLTP is also responsible for the content and transfer of vitamin E in cells and tissues (29), and vitamin E has been thought to regulate RNA synthesis (46). More investigations are needed to evaluate the potential of PLTP as a transcription regulator upon its lipid transfer property. It is remarkable that although flAPP was decreased in the membranous extracts, ADAM10 and CTFα were not changed by PLTP deficiency, which suggested that PLTP had no impact on the α-secretase-mediated non-amyloidogenic pathway, or there could been involvement of other events in addition to the non-amyloidogenic pathway.

PLTP deficiency in APP/PS1ΔE9 mice modulated autophagy

Growing evidence has demonstrated the impaired autophagosome-lysosomal degradation in AD, which could disrupt Aβ clearance and trigger AD pathology such as Aβ deposition (47). Surprisingly, impaired autophagy, namely, the elevated p62 and decreased ratio of LC3II to LC3I, was unfolded in the PLTP-deficient APP mice at the non-demented age. We also found a decrease of PI in the APP&PLTPko mice. The homolog phospholipids of PI, such as PI3P and PI(3,5)P_2, have been demonstrated to play a fundamental role in various aspects of autophagy, including the maturation and turnover of autophagosomes (48), suggesting the potential of PLTP in modulating autophagy. Besides, sphingosine-1-phosphate (S1P), a potent sphingolipid second messenger, is also implicated in numerous cellular processes including autophagy (49,50), and the content of S1P is decreased in PLTP-deficient mice (51). In general, with the capacity for brain lipid homeostasis, PLTP might play an important role in autophagy modulation and the related intracellular clearance of Aβ.

Down-regulated BDNF level by PLTP deficiency related to Aβ42

BDNF, which contributes to the survival of neuron and synapse, has often been correlated with memory and dementia (52,53). In this study, we found that BDNF was decreased in APP&PLTPko mice with impaired cognition, which indicated a causative role of BDNF in PLTP deficiency-induced memory dysfunction. Further, we determined a specific negative correlation between BDNF and the Aβ42, not the Aβ40, consistent with the reported Aβ42 toxicity on decreased BDNF (54). Hence, the reduced BDNF level might be due to the elevated Aβ42 by PLTP deficiency. In contrast, the neuroprotective effect of BDNF can be mediated by the up-regulation of autophagy (55). Thus, impaired autophagy via PLTP deficiency might be partially caused by down-regulated BDNF, which was critical for the accelerated memory dysfunction.

In conclusion, our current study presented a novel model with early onset of cognitive dysfunction by PLTP deficiency in APP/PS1ΔE9 mice without appearance of amyloid deposition. Dysfunction of PLTP might be a risk factor for the elevated Aβ in the preclinical stage of AD. We first found several potential functions of PLTP deficiency in the AD model mice: impairing cognitive performance; involvement in APP trafficking/processing and intracellular Aβ generation; inducing Aβ42-related alteration of BDNF and disturbing levels of p62 and LC3 in autophagy. We presented a novel model to link phospholipid metabolism to APP processing. These established PLTP-deficient AD mouse

models could provide insights into early stages in AD such as MCI or preclinical AD.

Materials and Methods

Animals

All mice were on the homogeneous C57BL/6 background. PLTP-deficient mice (PLTP knockout homozygote, PLTPko mice for short) were generated by Dr X.C. Jiang's laboratory (56). APP/PS1ΔE9 transgenic mice (APP/PS1ΔE9 heterozygote, bought from Institute of Laboratory Animal Science, Chinese Academy of Medical Science, abbreviated as APP mice for convenience), a well-characterized AD mice model (31), express human APP with Swedish mutation (APPsw) and human PS1 (presenilin 1) with deletion in exon 9 (PS1ΔE9). APP/PS1ΔE9 mice were cross-bred to PLTPko mice to generate APP/PS1ΔE9&PLTPko mice (APP/PS1ΔE9 heterozygote and PLTP knockout homozygote, APP&PLTPko mice for short). APP mice with wild-type mouse PLTP (referred to as APP mice) were used as controls. In addition, for behavioral tests, we used non-transgenic wild-type (WT mice) and PLTPko mice. All mice were matched for sex and used at the age of 3 months ± 1 week. Mice were maintained in a pathogen-free facility on a 12 h light/dark cycle with water and food provided *ad libitum*. All work was approved by the Peking University Biomedical Ethics Committee Experimental Animal Ethics Branch.

MWM

Behavior assessment was performed with a modified version of the MWM used to assess spatial navigation learning and memory retention as described (57,58) with minor modifications.

Initially, mice received a habituation trial to explore the pool of water (diameter 150 cm, height 40 cm and temperature 23 ± 1°C) without the platform present. Following habituation, visible platform training was performed for 2 consecutive days to measure the motivation of the mice to find a platform, visual acuity of the mice and the ability of mice to use local cues. In the acquisition phase, we measured the ability of mice to form a representation of the spatial relationship between a safe, but invisible (submerged 1 cm below the water level), platform (10 cm in diameter) and visual cues surrounding the maze. Animals were allowed 60 s to locate the platform and 20 s to rest on it. Mice that failed to find the platform were led there by the experimenter and allowed to rest there for 20 s. Twenty-four hours following the last acquisition trial, a single 60 s probe trial was administered to assess spatial memory retention. For the probe trial, animals were returned to the maze, but with no platform present, and parameters were recorded to assess the ability of the mouse to remember the previous location of the platform.

There was no significant difference in the swimming speed among all groups (WT mice: 8.27 ± 0.15 cm/s, $n = 12$; PLTPko mice: 8.33 ± 0.17 cm/s, $n = 9$; APP mice: 8.08 ± 0.13 cm/s, $n = 11$ and APP&PLTPko mice: 8.12 ± 0.26 cm/s, $n = 11$). There was no difference in the visual cue test either (data not shown), suggesting that all mice did not have visual problems.

Y-maze test

Spatial memory was also assessed in a Y-maze task as described (59) with minor modifications. The Y-maze apparatus was made up of three enclosed black plexiglass arms (50 cm long, 11 cm wide and 10 cm high) with extra-maze visual cues around the maze. In the first training (acquisition) trial, mice were placed at the end of a pseudo-randomly chosen start arm and allowed to explore the maze for 5 min with one of the arms closed (novel arm). Mice were returned to their home cage until the second (retrieval) trial. During the retrieval trial, the novel arm was opened and the mice were once again placed at the start arm and allowed to explore freely the three arms for 5 min. The number of entries in each arm, especially the novel arm, was recorded. Entry into an arm was defined as placement of all four paws into the arm.

Animal tissue processing

Mice were anesthetized by intraperitoneal injection of chloral hydrate (5%) and perfused transcardially with 25 ml of cold 0.1 M phosphate-buffered saline (PBS) (pH 7.4) each. For western blot analysis, brains were rapidly removed and divided into hemispheres, and in each of the hemispheres, the cortex and hippocampus were separated from other brain structures. These brain structures were snap-frozen on dry ice and stored at −80°C until use. For immunohistochemistry, whole brains were drop-fixed in 4% paraformaldehyde at 4°C for 48 h before storage in 30% sucrose.

Cellular fractionation

Preparation of membrane and cytoplasmic fractions was carried out as described previously (60,61), with minor modifications for the quantification of APP in the subcellular compartments. Briefly, a modified lysis buffer was used containing Tris–HCl 25 mM pH 7.4, ethylenediaminetetraacetic acid 2 mM, ethyleneglycoltetraacetic acid (EGTA) 1 mM, phenylmethylsulfonyl fluoride 0.1 mM and a complete set of protease inhibitors; after centrifugation for 3 min at 4°C and 3000*g* to separate the nuclei, cell lysates were further pelleted by centrifugation for 50 min at 4°C and 100 000*g*. The resulting pellet (referred to here as the membranous extract) was resuspended in the lysis buffer. The supernatants were referred as the cytoplasmic extract (intracellular compartment). In each subcellular extract, the proteins (immature APP, mature APP and β-actin) were determined by western blot analysis.

Western blot analysis

The frozen hemibrains (only cortices and hippocampi) were homogenized and lysed on ice in western blot lysis buffer containing 50 mM Tris–HCl, pH 6.8, 8 M urea, 5% β-mercaptoethanol, 2% sodium dodecyl sulfate (SDS) and protease inhibitors. The lysates were collected, centrifuged at 12 000*g* at 4°C for 5 min and quantified for the total proteins with the BCA protein assay kit. For western blot analysis, total proteins and proteins in subcellular compartments were separated on 10% T, 5% C bicine/Tris, 8 M urea, SDS–polyacrylamide gel electrophoresis (PAGE) or 10–18% regular SDS–PAGE system (62,63). Briefly, protein was transferred to 0.45 μm polyvinylidene difluoride membranes (Immobilon-P; Millipore, Bedford, MA, USA), blocked for 1 h in 5% (m/v) non-fat milk in Tris-buffered saline (pH 7.5) and supplemented with 0.1% Tween 20. Antibodies and their dilutions used in this study included A8717 (1:10 000, Sigma, St Louis, MO, USA) for flAPP and APP derivatives in total proteins (62), WO-2 (1:1000, Millipore) for APP maturation (64), BACE1 mAb (1:2000, R&D, Minneapolis, MN, USA), ADAM10 (1:2000, Abcam, Cambridge, MA, USA), presenilin-1 mAb (1:1000, CHEMICON International, Billerica, MA, USA), BDNF pAb (1:1000, Millipore), p62 (1:2000, Medical & Biological Laboratories Co.), LC3 (1:1000, Novus

Biologicals) and β-actin mAb (1:5000, Sigma) as an internal reference control. Following incubation with the appropriate horseradish peroxidase-conjugated secondary antibody for 1 h at room temperature, the immunoblots were developed using the ECL system. Quantitative densitometric analyses were performed with Quantity One software (Bio-Rad, Hercules, CA, USA). Representative blots from at least three independent experiments were shown.

β-secretase activity assay

β-secretase activity in the brain tissues was determined using a commercially available β-secretase activity kit (Abcam). Briefly, protein was extracted from brain tissues using ice-cold extraction buffer, incubated on ice for 10 min and centrifuged for 5 min at 4°C and 10 000*g*. The supernatants were collected, and the protein concentrations were quantified by the BCA method and equal amount of cellular proteins was used for the measurement of β-secretase activity (65). An aliquot of 50 μl of blank, standards or samples, 50 μl of 2× reaction buffer and 2 μl of β-secretase substrate were added to each well and incubated in the dark at 37°C for 2 h. With a multi-functional microplate reader (Infinity F200, TECAN, Switzerland), fluorescence intensity was read at excitation and emission wavelengths of 355 and 510 nm, respectively.

Quantification of Aβ peptide levels by sandwich ELISA

The fresh-frozen mouse hemibrains (only cortices and hippocampi) were serially homogenized into detergent-soluble fractions as described (66). All samples were assayed for Aβ40 and Aβ42 by sandwich ELISA, according to the manufacturer's instructions (Biosource International, Camarillo, CA, USA). The detection limit of ELISA was 0.1 fmol/ml for Aβ40 and 0.2 fmol/ml for Aβ42. The Aβ concentration was normalized to the weight of the hemibrains. All measurements were performed in duplicate.

Immunohistochemistry and confocal microscopy

Tissue preparation and immunohistochemistry were performed as described (67) with minor modifications. Free-floating sections (18 μm thick) were processed for free-floating immunohistochemistry. Primary antibodies for Aβ (6E10, 1:100) (6), APP (A8717, Sigma, 1:500), Tuj-1 (MMS-435P, Covance, 1:500), PLTP (sc-30835, Santa Cruz, 1:100), Rab5 (sc-309, Santa Cruz, 1:100), Rab7 (sc-6563, Santa Cruz, 1:100), p62 (1:200, PM045, Medical & Biological Laboratories Co.) and LC3 (1:100, NB100-2220, Novus Biologicals) were applied overnight at 4°C. Secondary antibodies used were Alexa Fluor 488-labeled donkey anti-mouse IgG (MicroProbe, 1:2000), Alexa Fluor 568-labeled goat anti-mouse IgG (MicroProbe, 1:2000), Alexa Fluor 594-labeled goat anti-rabbit IgG (MicroProbe, 1:2000) and Alexa Fluor 488-labeled donkey anti-goat IgG (MicroProbe, 1:1000). Cell nuclei were counterstained with Hoechst 33258 (Invitrogen, Carlsbad, CA, USA). Fluorescence images were acquired with a confocal laser scanning microscope (LSM510; Carl Zeiss Co., Oberkochen, Germany). No fluorescence was detected with the primary antibody omitted.

Cell culture and immunofluorescence

Mouse N2a neuroblastoma cells stably expressing Swedish mutant APP (abbreviated as APPsw-N2a cells for convenience) were kindly provided by Drs Sangram S. Sisodia and SeongHun Kim (University of Chicago) (68) and were maintained in normal Dulbecco's modified Eagle's medium and supplemented with 10% fetal bovine serum. Immunofluorescence was carried out as described previously (61). Cells on cover slips were fixed with 4% paraformaldehyde in PBS for 20 min at room temperature, permeabilized with 0.3% Triton X-100/PBS for 5 min and blocked with 10% bovine serum albumin in PBS. Primary antibodies for APP (A8717, Sigma, 1:500) and PLTP (sc-30835, Santa Cruz, 1:100) were applied overnight at 4°C. Secondary antibodies used were Alexa Fluor 594-labeled goat anti-rabbit IgG (MicroProbe, 1:2000) and Alexa Fluor 488-labeled donkey anti-goat IgG (MicroProbe, 1:1000). Cell nuclei were counterstained with Hoechst 33258 (Invitrogen). Confocal fluorescence images were acquired as described earlier.

Reverse transcriptase–PCR analysis

Total RNA was extracted with TRIZOL (Invitrogen) and converted to cDNA by reverse transcriptase (RT) using random hexamers to prime superscript III RNasefree RT (Invitrogen), according to the manufacturer's instructions. RT–PCR primers used in this study were as follows: human APP sense primer, 5′-GCTGGAGGT ACCCACTGATG-3′; human APP antisense primer, 5′-GCACCA GTTCTGGATGGTCA-3′; BACE1 sense primer, 5′-CTGCAAGGAG ACGGAGAAGT-3′; BACE1 antisense primer, 5′-GGCTCGATCGAA GACGACAT-3′; GAPDH sense primer, 5′-GGAGAGTGTTTCCTCGT CCC-3′; GAPDH antisense primer, 5′-ACTGTGCCGTTGAATTT GCC-3′; ADAM10 sense primer, 5′-CTCTTTGCAGTGGAGCAAG C-3′; ADAM10 antisense primer, 5′-CACCAGTGAGCCACAATCCA-3′; presenilin-1 sense primer, 5′-TGGTGAAACTCTGCGTCTGG-3′ and presenilin-1 antisense primer, 5′-GCTGTCTTGTGTTGG TTCCTCA-3′. PCRs were performed at 94°C for 30 s, 55°C for 1 min and 68°C for 2 min during 40 cycles, followed by a final extension of 7 min at 68°C (69).

Co-immunoprecipitation and immunoblot analysis

Mouse brain tissue from APP mice was homogenized and lysed in lysis buffer [50 mM Tris (pH 7.4), 150 mM NaCl and 1% Nonidet P-40], containing a complete protease inhibitor mixture (Roche). The immunoprecipitation was performed as described (70) with minor modifications. Whole brain extract proteins were used for immunoprecipitation with the indicated antibodies for PLTP and APP. Briefly, 4 μg of antibody was added into 1 ml of brain extract, which was then incubated at 4°C overnight. After the addition of Protein G-agarose beads (GE Healthcare), the incubation was continued for 4 h at 4°C. The resulting immunoprecipitates were extensively washed with lysis buffer for three times and eluted with SDS loading buffer by boiling for 5 min. Samples were separated by 10–12% SDS–PAGE and transferred to nitrocellulose membranes for immunoblot analysis with the indicated antibodies. Data were collected from at least three independent experiments.

Shotgun lipidomics analysis of brain lipids

Shotgun lipidomics analysis of brain lipids was performed, as described previously (28). Lipids were extracted from dissected brain tissues by the modified Bligh and Dyer method as described (28). A triple–quadrupole mass spectrometer equipped with a Namomate device and Xcalibur system was used to analyze lipids in the brain extract. Xcalibur analysis software was applied to analyze all tandem mass spectrometry data automatically acquired by a customized sequence. For each brain tissue sample, internal standards were added to quantify individual molecular species of lipid classes.

Statistical analysis

Analyses were conducted using GraphPad Prism 5 for Windows (GraphPad Software, San Diego, CA, USA). Comparisons among multiple groups were made by one-way analysis of variance (ANOVA), followed by a Tukey's *post hoc* test, and the Student's *t*-test was used for comparisons between two groups. Statistical significance of differences between mean scores during the acquisition phase of training in the MWM was assessed with two-way repeated-measures ANOVA (general linear model/RM-ANOVA) and Tukey's *post hoc* analysis for multiple comparisons using group and trial block number as sources of variation. $P < 0.05$ was regarded as statistically significant (two-tailed tests).

Supplementary Material

Supplementary Material is available at *HMG* online.

Acknowledgement

The authors thank Prof. Xuemin Xu for the analysis technique of APP processing.

Conflict of Interest statement. All the authors declare no conflict of interest.

Funding

This work was supported by the National High Technology Research and Development Program of China (973 Program nos 2012CB911000 and 2012CB911004) and the National Natural Science Foundation of China (NSFC; Grant nos 81171015, 81371205 and 61450004).

References

1. Fleisher, A.S., Chen, K., Quiroz, Y.T., Jakimovich, L.J., Gomez, M.G., Langois, C.M., Langbaum, J.B., Ayutyanont, N., Roontiva, A., Thiyyagura, P. *et al.* (2012) Florbetapir PET analysis of amyloid-beta deposition in the presenilin 1 E280A autosomal dominant Alzheimer's disease kindred: a cross-sectional study. *Lancet Neurol.*, **11**, 1057–1065.
2. Zhang, X. and Song, W. (2013) The role of APP and BACE1 trafficking in APP processing and amyloid-beta generation. *Alzheimers Res. Ther.*, **5**, 46.
3. Zhou, Z.D., Chan, C.H., Ma, Q.H., Xu, X.H., Xiao, Z.C. and Tan, E.K. (2011) The roles of amyloid precursor protein (APP) in neurogenesis: implications to pathogenesis and therapy of Alzheimer disease. *Cell Adhes. Migr.*, **5**, 280–292.
4. Shrivastava-Ranjan, P., Faundez, V., Fang, G., Rees, H., Lah, J.J., Levey, A.I. and Kahn, R.A. (2008) Mint3/X11gamma is an ADP-ribosylation factor-dependent adaptor that regulates the traffic of the Alzheimer's precursor protein from the trans-Golgi network. *Mol. Biol. Cell*, **19**, 51–64.
5. Tseng, B.P., Kitazawa, M. and LaFerla, F.M. (2004) Amyloid beta-peptide: the inside story. *Curr. Alzheimer Res.*, **1**, 231–239.
6. Billings, L.M., Oddo, S., Green, K.N., McGaugh, J.L. and LaFerla, F.M. (2005) Intraneuronal Abeta causes the onset of early Alzheimer's disease-related cognitive deficits in transgenic mice. *Neuron*, **45**, 675–688.
7. Vuletic, S., Jin, L.W., Marcovina, S.M., Peskind, E.R., Moller, T. and Albers, J.J. (2003) Widespread distribution of PLTP in human CNS: evidence for PLTP synthesis by glia and neurons, and increased levels in Alzheimer's disease. *J. Lipid Res.*, **44**, 1113–1123.
8. Albers, J.J., Vuletic, S. and Cheung, M.C. (2012) Role of plasma phospholipid transfer protein in lipid and lipoprotein metabolism. *Biochim. Biophys. Acta*, **1821**, 345–357.
9. Jauhiainen, M., Huuskonen, J., Baumann, M., Metso, J., Oka, T., Egashira, T., Hattori, H., Olkkonen, V.M. and Ehnholm, C. (1999) Phospholipid transfer protein (PLTP) causes proteolytic cleavage of apolipoprotein A-I. *J. Lipid Res.*, **40**, 654–664.
10. Vuletic, S., Dong, W., Wolfbauer, G., Day, J.R. and Albers, J.J. (2009) PLTP is present in the nucleus, and its nuclear export is CRM1-dependent. *Biochim. Biophys. Acta*, **1793**, 584–591.
11. Wang, H., Yu, Y., Chen, W., Cui, Y., Luo, T., Ma, J., Jiang, X.C. and Qin, S. (2014) PLTP deficiency impairs learning and memory capabilities partially due to alteration of amyloid-beta metabolism in old mice. *J. Alzheimers Dis.*, **39**, 79–88.
12. Desrumaux, C., Pisoni, A., Meunier, J., Deckert, V., Athias, A., Perrier, V., Villard, V., Lagrost, L., Verdier, J.M. and Maurice, T. (2013) Increased amyloid-beta peptide-induced memory deficits in phospholipid transfer protein (PLTP) gene knockout mice. *Neuropsychopharmacology*, **38**, 817–825.
13. Lalonde, R., Kim, H.D. and Fukuchi, K. (2004) Exploratory activity, anxiety, and motor coordination in bigenic APPswe + PS1/DeltaE9 mice. *Neurosci. Lett.*, **369**, 156–161.
14. Walsh, D.M., Klyubin, I., Fadeeva, J.V., Cullen, W.K., Anwyl, R., Wolfe, M.S., Rowan, M.J. and Selkoe, D.J. (2002) Naturally secreted oligomers of amyloid beta protein potently inhibit hippocampal long-term potentiation *in vivo*. *Nature*, **416**, 535–539.
15. Sato, N. and Morishita, R. (2013) Plasma abeta: a possible missing link between Alzheimer disease and diabetes. *Diabetes*, **62**, 1005–1006.
16. Zhang, W., Bai, M., Xi, Y., Hao, J., Zhang, Z., Su, C., Lei, G., Miao, J. and Li, Z. (2012) Multiple inflammatory pathways are involved in the development and progression of cognitive deficits in APPswe/PS1dE9 mice. *Neurobiol. Aging*, **33**, 2661–2677.
17. Pedros, I., Petrov, D., Allgaier, M., Sureda, F., Barroso, E., Beas-Zarate, C., Auladell, C., Pallas, M., Vazquez-Carrera, M., Casadesus, G. *et al.* (2014) Early alterations in energy metabolism in the hippocampus of APPswe/PS1dE9 mouse model of Alzheimer's disease. *Biochim. Biophys. Acta*, **1842**, 1556–1566.
18. Sisodia, S.S. (1992) Beta-amyloid precursor protein cleavage by a membrane-bound protease. *Proc. Natl Acad. Sci. USA*, **89**, 6075–6079.
19. Koo, E.H. and Squazzo, S.L. (1994) Evidence that production and release of amyloid beta-protein involves the endocytic pathway. *J. Biol. Chem.*, **269**, 17386–17389.
20. Choy, R.W., Cheng, Z. and Schekman, R. (2012) Amyloid precursor protein (APP) traffics from the cell surface via endosomes for amyloid beta (Abeta) production in the trans-Golgi network. *Proc. Natl Acad. Sci. USA*, **109**, E2077–E2082.
21. Peng, S., Wuu, J., Mufson, E.J. and Fahnestock, M. (2005) Precursor form of brain-derived neurotrophic factor and mature brain-derived neurotrophic factor are decreased in the pre-clinical stages of Alzheimer's disease. *J. Neurochem.*, **93**, 1412–1421.
22. Michalski, B. and Fahnestock, M. (2003) Pro-brain-derived neurotrophic factor is decreased in parietal cortex in Alzheimer's disease. *Brain Res. Mol. Brain Res.*, **111**, 148–154.
23. Li, G., Peskind, E.R., Millard, S.P., Chi, P., Sokal, I., Yu, C.E., Bekris, L.M., Raskind, M.A., Galasko, D.R. and Montine, T.J. (2009) Cerebrospinal fluid concentration of brain-derived neurotrophic factor and cognitive function in non-demented subjects. *PLoS ONE*, **4**, e5424.

24. Ciaramella, A., Salani, F., Bizzoni, F., Orfei, M.D., Langella, R., Angelucci, F., Spalletta, G., Taddei, A.R., Caltagirone, C. and Bossu, P. (2013) The stimulation of dendritic cells by amyloid beta 1–42 reduces BDNF production in Alzheimer's disease patients. *Brain Behav. Immun.*, **32**, 29–32.
25. Christensen, R., Marcussen, A.B., Wortwein, G., Knudsen, G. M. and Aznar, S. (2008) Abeta(1–42) injection causes memory impairment, lowered cortical and serum BDNF levels, and decreased hippocampal 5-HT(2A) levels. *Exp. Neurol.*, **210**, 164–171.
26. Yu, W.H., Cuervo, A.M., Kumar, A., Peterhoff, C.M., Schmidt, S.D., Lee, J.H., Mohan, P.S., Mercken, M., Farmery, M.R., Tjernberg, L.O. *et al.* (2005) Macroautophagy—a novel beta-amyloid peptide-generating pathway activated in Alzheimer's disease. *J. Cell Biol.*, **171**, 87–98.
27. Nixon, R.A. (2007) Autophagy, amyloidogenesis and Alzheimer disease. *J. Cell Sci.*, **120**, 4081–4091.
28. Cheng, H., Jiang, X. and Han, X. (2007) Alterations in lipid homeostasis of mouse dorsal root ganglia induced by apolipoprotein E deficiency: a shotgun lipidomics study. *J. Neurochem.*, **101**, 57–76.
29. Desrumaux, C., Risold, P.Y., Schroeder, H., Deckert, V., Masson, D., Athias, A., Laplanche, H., Le Guern, N., Blache, D., Jiang, X.C. *et al.* (2005) Phospholipid transfer protein (PLTP) deficiency reduces brain vitamin E content and increases anxiety in mice. *FASEB J.*, **19**, 296–297.
30. Zhou, T., He, Q., Tong, Y., Zhan, R., Xu, F., Fan, D., Guo, X., Han, H., Qin, S. and Chui, D. (2014) Phospholipid transfer protein (PLTP) deficiency impaired blood–brain barrier integrity by increasing cerebrovascular oxidative stress. *Biochem. Biophys. Res. Commun.*, **445**, 352–356.
31. Webster, S.J., Bachstetter, A.D., Nelson, P.T., Schmitt, F.A. and Van Eldik, L.J. (2014) Using mice to model Alzheimer's dementia: an overview of the clinical disease and the preclinical behavioral changes in 10 mouse models. *Front. Genet.*, **5**, 88.
32. Gouras, G.K., Tsai, J., Naslund, J., Vincent, B., Edgar, M., Checler, F., Greenfield, J.P., Haroutunian, V., Buxbaum, J.D., Xu, H. *et al.* (2000) Intraneuronal Abeta42 accumulation in human brain. *Am. J. Pathol.*, **156**, 15–20.
33. Fernandez-Vizarra, P., Fernandez, A.P., Castro-Blanco, S., Serrano, J., Bentura, M.L., Martinez-Murillo, R., Martinez, A. and Rodrigo, J. (2004) Intra- and extracellular Abeta and PHF in clinically evaluated cases of Alzheimer's disease. *Histol. Histopathol.*, **19**, 823–844.
34. LaFerla, F.M., Green, K.N. and Oddo, S. (2007) Intracellular amyloid-beta in Alzheimer's disease. *Nat. Rev. Neurosci.*, **8**, 499–509.
35. Leon, W.C., Canneva, F., Partridge, V., Allard, S., Ferretti, M.T., DeWilde, A., Vercauteren, F., Atifeh, R., Ducatenzeiler, A., Klein, W. *et al.* (2010) A novel transgenic rat model with a full Alzheimer's-like amyloid pathology displays pre-plaque intracellular amyloid-beta-associated cognitive impairment. *J. Alzheimers Dis.*, **20**, 113–126.
36. Chui, D.H., Tanahashi, H., Ozawa, K., Ikeda, S., Checler, F., Ueda, O., Suzuki, H., Araki, W., Inoue, H., Shirotani, K. *et al.* (1999) Transgenic mice with Alzheimer presenilin 1 mutations show accelerated neurodegeneration without amyloid plaque formation. *Nat. Med.*, **5**, 560–564.
37. Nishitsuji, K., Tomiyama, T., Ishibashi, K., Ito, K., Teraoka, R., Lambert, M.P., Klein, W.L. and Mori, H. (2009) The E693Delta mutation in amyloid precursor protein increases intracellular accumulation of amyloid beta oligomers and causes endoplasmic reticulum stress-induced apoptosis in cultured cells. *Am. J. Pathol.*, **174**, 957–969.
38. Umeda, T., Tomiyama, T., Sakama, N., Tanaka, S., Lambert, M. P., Klein, W.L. and Mori, H. (2011) Intraneuronal amyloid beta oligomers cause cell death via endoplasmic reticulum stress, endosomal/lysosomal leakage, and mitochondrial dysfunction *in vivo*. *J. Neurosci. Res.*, **89**, 1031–1042.
39. Pigino, G., Morfini, G., Atagi, Y., Deshpande, A., Yu, C., Jungbauer, L., LaDu, M., Busciglio, J. and Brady, S. (2009) Disruption of fast axonal transport is a pathogenic mechanism for intraneuronal amyloid beta. *Proc. Natl Acad. Sci. USA*, **106**, 5907–5912.
40. Takahashi, R.H., Milner, T.A., Li, F., Nam, E.E., Edgar, M.A., Yamaguchi, H., Beal, M.F., Xu, H., Greengard, P. and Gouras, G.K. (2002) Intraneuronal Alzheimer abeta42 accumulates in multivesicular bodies and is associated with synaptic pathology. *Am. J. Pathol.*, **161**, 1869–1879.
41. Vetrivel, K.S. and Thinakaran, G. (2010) Membrane rafts in Alzheimer's disease beta-amyloid production. *Biochim. Biophys. Acta*, **1801**, 860–867.
42. Lai, A., Sisodia, S.S. and Trowbridge, I.S. (1995) Characterization of sorting signals in the beta-amyloid precursor protein cytoplasmic domain. *J. Biol. Chem.*, **270**, 3565–3573.
43. Almenar-Queralt, A., Falzone, T.L., Shen, Z., Lillo, C., Killian, R.L., Arreola, A.S., Niederst, E.D., Ng, K.S., Kim, S.N., Briggs, S.P. *et al.* (2014) UV irradiation accelerates amyloid precursor protein (APP) processing and disrupts APP axonal transport. *J. Neurosci.*, **34**, 3320–3339.
44. Albi, E. and Viola Magni, M.P. (2004) The role of intranuclear lipids. *Biol. Cell.*, **96**, 657–667.
45. Hunt, A.N. (2006) Dynamic lipidomics of the nucleus. *J. Cell. Biochem.*, **97**, 244–251.
46. Guarnieri, C., Flamigni, F. and Caldarera, C.R. (1980) Subcellular localization of alpha-tocopherol and its effect on RNA synthesis in perfused rabbit heart. *Ital. J. Biochem.*, **29**, 176–184.
47. Salminen, A., Kaarniranta, K., Kauppinen, A., Ojala, J., Haapasalo, A., Soininen, H. and Hiltunen, M. (2013) Impaired autophagy and APP processing in Alzheimer's disease: the potential role of Beclin 1 interactome. *Prog. Neurobiol.*, **106–107**, 33–54.
48. Dall'Armi, C., Devereaux, K.A. and Di Paolo, G. (2013) The role of lipids in the control of autophagy. *Curr. Biol.*, **23**, R33–R45.
49. Cuvillier, O. (2007) Sphingosine kinase-1—a potential therapeutic target in cancer. *Anticancer Drugs*, **18**, 105–110.
50. Lavieu, G., Scarlatti, F., Sala, G., Carpentier, S., Levade, T., Ghidoni, R., Botti, J. and Codogno, P. (2008) Sphingolipids in macroautophagy. *Methods Mol. Biol.*, **445**, 159–173.
51. Yu, Y., Guo, S., Feng, Y., Feng, L., Cui, Y., Song, G., Luo, T., Zhang, K., Wang, Y., Jiang, X.C. *et al.* (2014) Phospholipid transfer protein deficiency decreases the content of S1P in HDL via the loss of its transfer capability. *Lipids*, **49**, 183–190.
52. Acheson, A., Conover, J.C., Fandl, J.P., DeChiara, T.M., Russell, M., Thadani, A., Squinto, S.P., Yancopoulos, G.D. and Lindsay, R.M. (1995) A BDNF autocrine loop in adult sensory neurons prevents cell death. *Nature*, **374**, 450–453.
53. Huang, E.J. and Reichardt, L.F. (2001) Neurotrophins: roles in neuronal development and function. *Annu. Rev. Neurosci.*, **24**, 677–736.
54. Garzon, D.J. and Fahnestock, M. (2007) Oligomeric amyloid decreases basal levels of brain-derived neurotrophic factor (BDNF) mRNA via specific downregulation of BDNF transcripts IV and V in differentiated human neuroblastoma cells. *J. Neurosci.*, **27**, 2628–2635.
55. Chen, A., Xiong, L.J., Tong, Y. and Mao, M. (2013) Neuroprotective effect of brain-derived neurotrophic factor mediated by

autophagy through the PI3K/Akt/mTOR pathway. *Mol. Med. Rep.*, **8**, 1011–1016.
56. Jiang, X.C., Bruce, C., Mar, J., Lin, M., Ji, Y., Francone, O.L. and Tall, A.R. (1999) Targeted mutation of plasma phospholipid transfer protein gene markedly reduces high-density lipoprotein levels. *J. Clin. Invest.*, **103**, 907–914.
57. Liu, Y., Ye, Z., Yang, H., Zhou, L., Fan, D., He, S. and Chui, D. (2010) Disturbances of soluble *N*-ethylmaleimide-sensitive factor attachment proteins in hippocampal synaptosomes contribute to cognitive impairment after repetitive formaldehyde inhalation in male rats. *Neuroscience*, **169**, 1248–1254.
58. Fitz, N.F., Cronican, A., Pham, T., Fogg, A., Fauq, A.H., Chapman, R., Lefterov, I. and Koldamova, R. (2010) Liver X receptor agonist treatment ameliorates amyloid pathology and memory deficits caused by high-fat diet in APP23 mice. *J. Neurosci.*, **30**, 6862–6872.
59. Sooy, K., Webster, S.P., Noble, J., Binnie, M., Walker, B.R., Seckl, J.R. and Yau, J.L. (2010) Partial deficiency or short-term inhibition of 11beta-hydroxysteroid dehydrogenase type 1 improves cognitive function in aging mice. *J. Neurosci.*, **30**, 13867–13872.
60. Zimmermann, M., Gardoni, F., Marcello, E., Colciaghi, F., Borroni, B., Padovani, A., Cattabeni, F. and Di Luca, M. (2004) Acetylcholinesterase inhibitors increase ADAM10 activity by promoting its trafficking in neuroblastoma cell lines. *J. Neurochem.*, **90**, 1489–1499.
61. Yu, Y., Zhou, L., Sun, M., Zhou, T., Zhong, K., Wang, H., Liu, Y., Liu, X., Xiao, R., Ge, J. *et al.* (2012) Xylocoside G reduces amyloid-beta induced neurotoxicity by inhibiting NF-kappaB signaling pathway in neuronal cells. *J. Alzheimers Dis.*, **30**, 263–275.
62. Tong, Y., Yang, H., Tian, X., Wang, H., Zhou, T., Zhang, S., Yu, J., Zhang, T., Fan, D., Guo, X. *et al.* (2014) High manganese, a risk for Alzheimer's disease: high manganese induces amyloid-beta related cognitive impairment. *J. Alzheimers Dis.*, **42**, 865–878.
63. Zhao, G., Mao, G., Tan, J., Dong, Y., Cui, M.Z., Kim, S.H. and Xu, X. (2004) Identification of a new presenilin-dependent zeta-cleavage site within the transmembrane domain of amyloid precursor protein. *J. Biol. Chem.*, **279**, 50647–50650.
64. Spoerri, L., Vella, L.J., Pham, C.L., Barnham, K.J. and Cappai, R. (2012) The amyloid precursor protein copper binding domain histidine residues 149 and 151 mediate APP stability and metabolism. *J. Biol. Chem.*, **287**, 26840–26853.
65. Zhang, Q., Yang, G., Li, W., Fan, Z., Sun, A., Luo, J. and Ke, Z.J. (2011) Thiamine deficiency increases beta-secretase activity and accumulation of beta-amyloid peptides. *Neurobiol. Aging*, **32**, 42–53.
66. Takeda, S., Sato, N., Uchio-Yamada, K., Sawada, K., Kunieda, T., Takeuchi, D., Kurinami, H., Shinohara, M., Rakugi, H. and Morishita, R. (2010) Diabetes-accelerated memory dysfunction via cerebrovascular inflammation and Abeta deposition in an Alzheimer mouse model with diabetes. *Proc. Natl Acad. Sci. USA*, **107**, 7036–7041.
67. Xian, X., Liu, T., Yu, J., Wang, Y., Miao, Y., Zhang, J., Yu, Y., Ross, C., Karasinska, J.M., Hayden, M.R. *et al.* (2009) Presynaptic defects underlying impaired learning and memory function in lipoprotein lipase-deficient mice. *J. Neurosci.*, **29**, 4681–4685.
68. Kim, S.H., Leem, J.Y., Lah, J.J., Slunt, H.H., Levey, A.I., Thinakaran, G. and Sisodia, S.S. (2001) Multiple effects of aspartate mutant presenilin 1 on the processing and trafficking of amyloid precursor protein. *J. Biol. Chem.*, **276**, 43343–43350.
69. Pardossi-Piquard, R., Petit, A., Kawarai, T., Sunyach, C., Alves da Costa, C., Vincent, B., Ring, S., D'Adamio, L., Shen, J., Muller, U. *et al.* (2005) Presenilin-dependent transcriptional control of the Abeta-degrading enzyme neprilysin by intracellular domains of betaAPP and APLP. *Neuron*, **46**, 541–554.
70. Zhang, P., Tu, B., Wang, H., Cao, Z., Tang, M., Zhang, C., Gu, B., Li, Z., Wang, L., Yang, Y. *et al.* (2014) Tumor suppressor p53 cooperates with SIRT6 to regulate gluconeogenesis by promoting FoxO1 nuclear exclusion. *Proc. Natl Acad. Sci. USA*, **111**, 10684–10689.